Journal of Geochemical Exploration 175 (2017) 148–155

Contents lists available at ScienceDirect

Journal of Geochemical Exploration

journal homepage: www.elsevier.com/locate/gexplo

The geochemical characteristics of dust material and dust sources identification in northwestern China

Zhengcai Zhang [a,*], Zhibao Dong [a], Caixia Zhang [a], Guangqian Qian [a], Chunying Lei [b]

[a] Key Laboratory of Desert and Desertification, Cold and Arid Regions Environmental and Engineering Research Institute, Chinese Academy of Sciences, Lanzhou 730000, China
[b] Institute of Afforestation and Sand Control, Xinjiang Academy of Forestry Sciences, Urumqi 830063, China

ARTICLE INFO

Article history:
Received 5 January 2016
Revised 25 October 2016
Accepted 11 November 2016
Available online 12 November 2016

Keywords:
Geochemical
Trace element
Major element
Dust sources

ABSTRACT

To determine dust sources in the northwestern China, the spatial distribution of dust geochemical elements in the Hexi Corridor Desert, a total of 40 samples were collected at a height of 1.5 m over sandy and gravel surfaces at six field sites. In this work, 21 trace elements and seven major oxides were analyzed. Land surface characteristics influenced the dust emission, and the percentages of transported silt, clay, silt/sand, and clay/sand at a height of 1.5 m were related to gravel cover and the percentage of 0.063-mm-sized grains at the surface. The SiO_2 content was the highest (mean 61.20 ± 9.17%), whereas the K_2O content was the lowest (mean 1.9 ± 0.3%) in all field sites. For the six sites, the Ti content was the highest (mean 3247.5 ± 502.5 μg/g) and the Nb content was the lowest (mean 9.6 ± 1.9 μg/g). At all sites, Co, As, and Nd were enriched, whereas Mn, Ti, Sr, Ce, Ni, Rb, Y, P, V, Ga, and Ba were depleted. P, Ti, V, Ni, Rb, Sr, Y, Ba, and La originated from crustal sources, and Cl, Cr, Cu, and Zn were sensitive to anthropogenic activity. The main transported trace elements were Ti, Mn, Ba, P, Cl, Sr, and Zr, which accounted for >90% of the total trace elements. PCA analysis indicated that two principal components with eigenvalues > 1 could be extracted from the data. The relationship between Rb/Sr and Ba/Sr and between Fe/Al, Mg/Al, and Ca/Al was used to identify dust sources. Two dust sources were identified in northwestern China: one source comprised the Badain Jaran Desert, Tengger Desert, Hexi Corridor Desert, and part of the Inner Mongolian Gobi Desert, and the other source comprised the desert adjacent to Dunhuang Gobi Desert, and part of the Inner Mongolian Gobi Desert.

1. Introduction

Atmospheric dust particles have substantial effects on human activity and climate change. The desert and Gobi (gravel desert) regions in East Asia are considered to be dominant dust sources in Asia (Zhang et al., 1996; Kok et al., 2012; Zhang et al., 2016). The volume of dust from Asian dust sources accounts for approximately 70% of the total Asian sand emission (Zhang and Gong, 2005). However, the specific locations of dust sources are still under debate, largely due to a lack of detailed information on dust properties (such as composition and particle size distribution), unsound methodologies, and a lack of detailed field surface information. An understanding of the material compositions and chemical properties of dust is critical in identifying dust sources. Thus, dust geochemical properties have been widely used to identify dust sources (Zhang et al., 1996, 2003b; Sun et al., 2005; Zarasvandi et al., 2011; Reheis et al., 2002; Arimoto, 2001; Wang et al., 2011; Cesari et al., 2012; Abouchami et al., 2013). However, the lack of detailed data from dust source regions has hindered the progress of dust modeling research. Although many research studies (Table 1) have used mineralogical methods to establish dust occurrences, transport, and deposition, improvements are needed to achieve more quantitative mineralogical analyses (Arimoto, 2001).

In northwestern China, gravel and sandy deserts cover an area of approximately 130.8×10^4 km^2. Dunhuang is an important part of northwestern China, and as one of the major dust sources, this region has been the subject of substantial aeolian and atmospheric research (Zhang et al., 1996; Ta et al., 2003; Liu et al., 2004; Dong et al., 2011; Wang et al., 2012). However, despite the depth of research in this region, field observations on dust emission processes and transportation are lacking. Recently, based on our research regarding wind transport, we have suggested that this region may be a major source of dust, although we hesitate to conclude that Dunhuang is a source of dust that is transported over long distances. Therefore, we selected the sand and gravel deserts adjacent to Dunhuang as the study region. The aims of this study were to determine the spatial distribution and composition of chemical elements in the Dunhuang sandy desert and the adjacent gravel desert, to evaluate the spatial differences in the chemical element

* Corresponding author at: Cold and Arid Regions Environmental and Engineering Research Institute, Chinese Academy of Sciences, No. 260, West Donggang Road, Lanzhou, Gansu Province 730000, China.
E-mail address: zhangzhsi@sina.com (Z. Zhang).

http://dx.doi.org/10.1016/j.gexplo.2016.11.006
0375-6742/

Table 1
Previous geochemical methods used to identify dust sources.

Author	Geochemical parameters
Zhang et al. (1996)	Al, Fe, Mg, Sc, Fe/Al, Mg/Al, and Sc/Al
Zarasvandi et al. (2011)	Al, Fe, Mg, Sc, Fe/Al, Mg/Al, and Sc/Al
Sun et al. (2005)	Ca/Al
Wang et al. (2011)	Ca/Al

distributions, and to investigate the differences between chemical elements at the surface and in transported dust material. This study will provide useful reference data for modeling dust emission, transport, and deposition.

2. Study region and methods

2.1. Study region

To identify dust material sources, six field observation sites were established in an area in northwestern China with gravel and sandy deserts (Fig. 1a). This area included the northeastern area of the Kumtagh Desert and the adjacent gravel deserts. The gravel deserts are almost all distributed in the plateau area of the study region and can be divided into two types: erosion-deposition and deposition (Du, 1962). The six observation sites are Sanlongsha (Site 1), North desert (Site 2), Erdun (Site 3), Subei (Site 4), Liuyuan (Site 5), and Anxi (Site 6) (Fig. 1a, Table 2). The six sites were divided into the following four types: sandy desert (Site 2), gravel with sand (Sites 1 and 4), gravel with a crust (Site 6), and gravel without a crust (Sites 3 and 5) (Fig. S1). The observation period spanned from November 2013 to December 2014.

Table 2
Site locations and key surface parameters for the observation sites.

Site	Lat., N	Long., W	Mz	P[a]	G[b]	Crust
Site 1	40.677°	93.004°	0.83	0.47	9	No
Site 2	40.329°	92.576°	0.72	0.25	0	No
Site 3	40.146°	94.117°	0.22	10.01	23	Yes
Site 4	39.824°	94.479°	0.14	19.88	5	No
Site 5	40.660°	95.060°	0.26	10.70	87	No
Site 6	40.256°	95.188°	0.31	22.87	39	Yes

Mz, mean grain size (*mm*).
[a] P, Percentage < 0.063 mm (%).
[b] G, Gravel coverage (%).

2.2. Methods

Transported dust material was collected by a horizontal aeolian flux trap (Zhang et al., 2011; Zhang and Dong, 2014a, 2014b). The dust trap (Fig. 1b), which resembled the "Big Spring Number Eight" (BSNE) sampler developed by Fryrear (1986). In this paper, we installed the flux traps at heights of 0.25, 0.5, 1.0, and 1.5 m (Fig. 1b), and collected about 45 days period. The dust trap contains a bracket, a revolving chamber, and a wind vane to continually orient the trap parallel to the wind. More details about this trap can be found in Zhang et al. (2011). A streamlined collecting chamber was used to reduce airflow interference at the inlet. The dimensions of the collecting chamber were selected to reduce the airflow velocity so that the flow could exit through the top mesh screen. The airflow was also slow enough to ensure that dust was deposited through the bottom mesh into the loading chamber. The 850 μm mesh screen reduced the movement of the deposited material, it prevented collected material from breaking down, and it reduced any

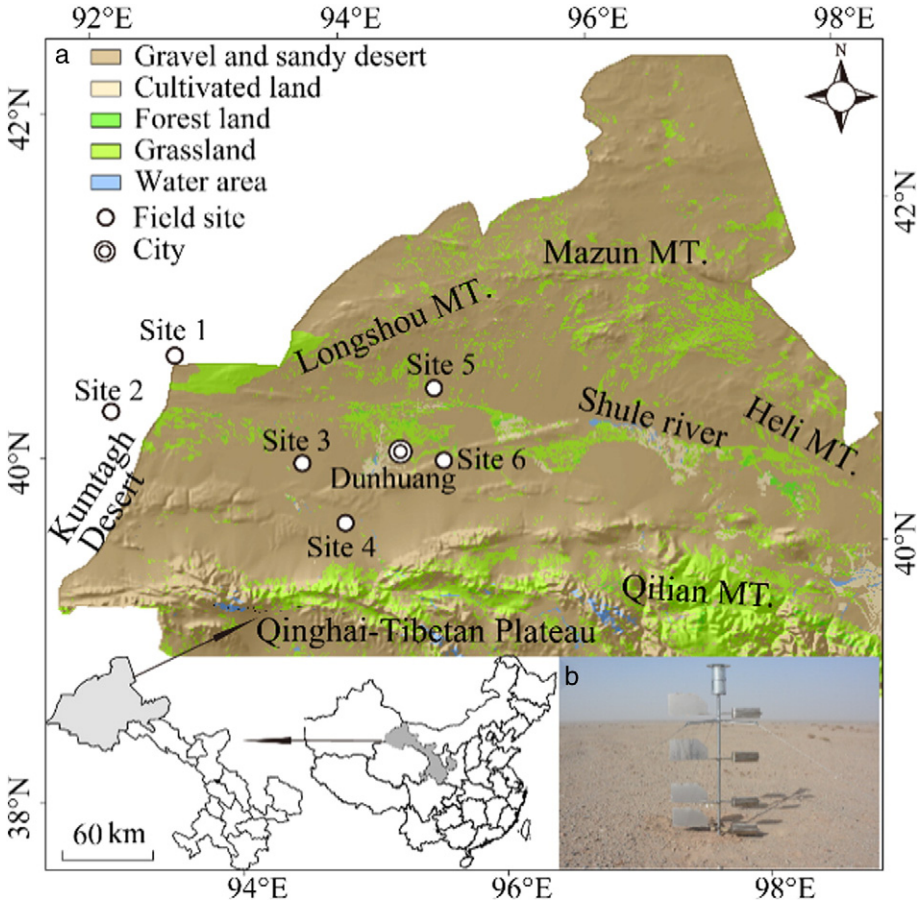

Fig. 1. (a) The study region and distribution of field observation sites. (b) The field measurements horizontal dust trap.

potential loss of the fine particles through the top of the screen. To collect dust from different directions, the revolving chamber was fitted with a wind vane that changed the direction of the sampler with changing wind directions. Six BSNE samplers were installed in the study region (Fig. 1a). The collected dust sediment were oven-dried before weighing. After each sampling period, the collecting chambers were removed from the dust trap, the collected dust sediment was removed for analysis, and the collecting chamber was then reset for next measurement. The dust sediment collected by the dust trap was weighed using an electronic balance with precision of 1 mg. A total of 40 measurements of dust emission quantity data were recorded. However, because severe dust storms occurred from April to June in northwestern China and lower collected sediment in others periods, we just analyzed the dust geochemical properties during this period (23 measurements). A total of 28 elements (SiO_2, Al_2O_3, Fe_2O_3, MgO, CaO, Na_2O, K_2O, Cl, P, Ti, V, Cr, Mn, Co, Ni, Cu, Zn, Ga, As, Rb, Sr, Y, Zr, Nb, Ba, Ce, Nd, and Pb) were measured by using a fully automated sequential wavelength dispersive X-ray fluorescence spectrometer(AXIOS, PANalytical B.V., Netherlands) with Super Sharp Tube of Rh-anode, 4.0 kW, 60 kV, 160 mA, 75 μ UHT Be end Window was used for elemental analysis at the Cold and Arid Regions Environmental and Engineering Research Institute, CAS. The software is SuperQ Version 5. The accessories include semi-auto press machine (ZHY-401A, Zhonghe corporation, Beijing), grinding mill with tungsten carbon (ZHM-1A, Zhonghe corporation, Beijing) and closed circuit cooling unit (BLK2-8FF-R, Zhonghe corporation, Beijing).

Before the experiments, the collected dust materials were crushed to <75 μm using a multipurpose grinder, and dried in an oven at 105 °C. 4 g of the dry powdered materials are pressed into a 32-mm-diameter pellet using 30-ton pressure using the pressed powder pellet technique. The briquettes were then stored in desiccators. After the XRF analysis, the dust geochemical concentration were established using the reference materials for rock (GBW07103 and GBW07114 (GSR01-GSR12)), GBW07120 and GBW07122 (GSR13 and GSR15), for soil (GBW07401 and GBW07408 (GSS01–GSS8)), GBW0743 and GBW07430 (GSS9–GSS16)), and for water sediment (GBW07301a and GBW07318 (GSD01–GSD14)). The measuring conditions were determined by the GB/T14506. 28–93 (Silicate rocks-Determination of contents of major and minor elements-X-ray fluorescence spectrometric methods).

The sand, silt and clay (grain sizes smaller than 1000 μm) contents of the collected samples were analyzed with a Malvern MasterSizer 2000 (Malvern Instruments Ltd., Malvern, England). This instrument measured sediment grain sizes ranging from 0.02 to 2000 μm.

The regression coefficients of the models were fitted using the MATLAB R2009a software (www.mathworks.com). Principal components analysis (PCA) is a useful statistical method for identifying possible source categories and has been used in dust research (Wang et al., 2012). Therefore, in this paper, we also used PCA to analyze the transported dust material at a height of 1.5 m.

3. Results

3.1. Transported grain size

Pye (1987) has found that particles smaller than 0.070 mm move as a suspension at heights > 1.5 m from the floor. Therefore, we analyzed the transported grain size at a height of 1.5 m (Fig. 2). There were obvious spatial distributions for the emission of silt and clay as well as for the ratios of silt/sand and clay/sand in the study region. The percentage of silt emission was highest at Site 6 (7.7%) and lowest at Site 1 (0%). The clay emission was similar to that of silt, which was highest at Site 6 (53.0%) and lowest at Site 1 (1.3%). At a height of 1.5 m, not all material can be transported long distances. Thus, we used the silt/sand and clay/dust to express the transported silt and clay (Fig. 2). At all sites, the percentage of silt in the sand was not >20%; however, the percentage of the clay was greater than the percentage of sand at some sites (such as Sites 5 and 6) (Fig. 2).

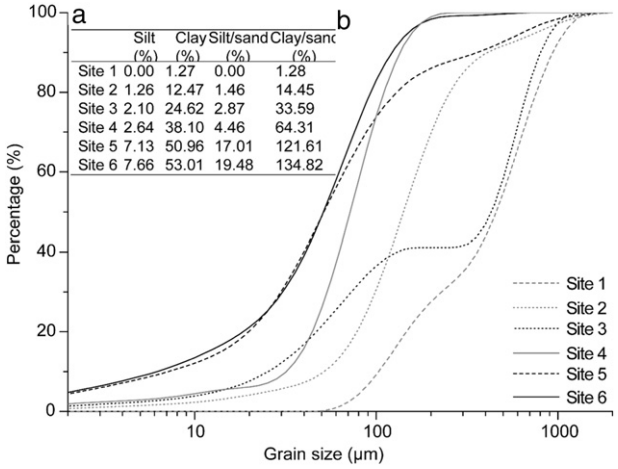

Fig. 2. Grain size distribution at a height of 1.5 m at six sites (a). Silt, clay, silt/sand, and clay/sand at a height of 1.5 m at six sites (b).

The surface characteristics (mean grain size, percentage of grains < 0.063 mm in size, gravel coverage and crust) influenced the transported silt and clay contents. The results of Sweeney et al. (2013) have indicated that sandy deserts are major dust sources and that gravel deserts are minor dust sources compared to eight other land surfaces (dry washes, dunes, playa margins, distal alluvial fans, lacustrine beaches, salt-crusted playas, silt–clay-crusted playas, and desert pavements). Our field observations indicate that gravel deserts (Sites 5 and 6) can provide more dust material than sand deserts (Site 2) according to the transported silt contents (Fig. 2). A multivariate correlation analysis indicated that the silt contents were closely related to gravel coverage (correlation coefficient = 0.80) and the percentage of grains < 0.063 mm in size (correlation coefficient = 0.69). The clay content was closely related to the percentage of grains < 0.063 mm in size (correlation coefficient = 0.84) and gravel coverage (correlation coefficient = 0.69). Although the percentages of silt, clay, silt/sand, and clay/sand had linear relationships with the percentage of grains <0.063 mm in size (Supplemental Fig. S2), the percentage of clay and the ratio of clay/sand had stronger relationships than the percentage of silt and the ratio of silt/sand.

3.2. Elemental composition

Although the transported dust material (grain size) were different (Fig. 2), our field observation indicated that the content of geochemical elements at the four height (0.25, 0.5, 1.0, and 1.5 m) were similar (Fig. 3, because of the similarity of all observation sites, we just selected Site 6 to show). Meanwhile, transported dust material at the 1.5 m height can be considered as long-term transported material. Therefore, to compare the variance of chemical elements in emitted dust between different sites, samples obtained at a height of 1.5 m were analyzed. A correlation analysis of 28 geochemical elements at the six observation sites indicated that Sites 1, 2, 3 and 4 had similar sources and that Sites 5 and 6 had similar sources (Table 3). The contents exhibited similar trends at the six sites. The main transported trace elements were Ti, Mn, Ba, P, Cl, Sr, and Zr, which accounted for >90% of the total trace elements. The percentage of Ti was largest for Sites 1, 2, 3, 4, and 6 (55, 55, 58, 47, and 37%, respectively), whereas for Site 5, the percentage of the trace element Cl was largest (51%). The percentage of Ba was the second largest for Sites 1, 2, 3, and 4 (9, 12, 7, and 8%, respectively); however, for Site 5, the percentage of the trace element Ti was highest (25%), and for Site 6, the percentage of the trace element Cl was highest (33%). For the major oxides, the SiO_2 content was the highest for the

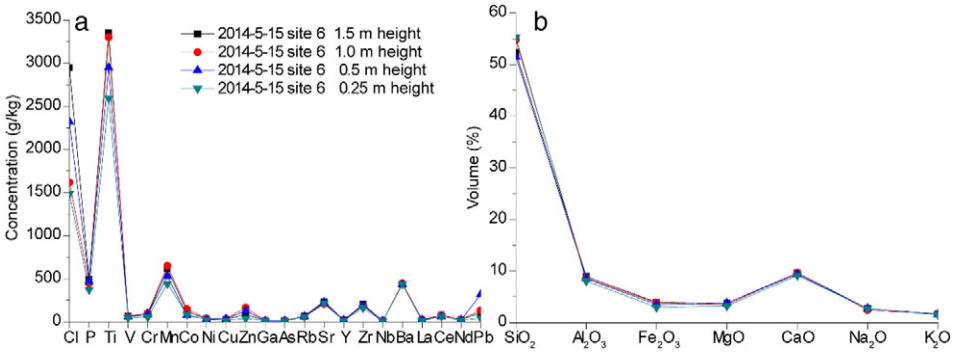

Fig. 3. Comparison of geochemical elements among four heights (0.25, 0.5, 1, and 1.5 m) at site 6 for trace elements (a) and major elements (b).

five sub-regions (ranging from 52.3% to 76.1%, mean 61.2 ± 9.2%) and the K_2O content was the lowest (ranging from 1.7% to 2.4%, mean 1.9 ± 0.3%). Our results are similar to those of a previous study, which found that SiO_2, Al_2O_3, Fe_2O_3, CaO, Ti, and Mn are the dominant elements in the geochemical composition of the Dunhuang dust material (Zhang et al., 2003b).

Fig. 4 shows the enrichments normalized to the composition of the upper continental crust (UCC, Taylor and McLennan, 1995). The normalized enrichments of trace elements could be divided into three types: (i) Co, As, and Nd were enriched at all sites; (ii) Mn, Ti, Sr, Ce, Ni, Rb, Y, P, V, Ga, and Ba were depleted at all sites; and (iii) Cl, Cr, Cu, Zn, Zr, Nb, and Pb were either enriched or depleted among the sites. Among the major elements, SiO_2 was enriched relative to the UCC at Sites 1 and 2 but depleted at the other sites, whereas Al_2O_3, Fe_2O_3, Na_2O, and K_2O were depleted at all sites. Our results are similar to those of a previous study on the surface geochemical properties in the Kumtagh Desert and the adjacent gravel regions: MgO and CaO were enriched on gravel surfaces and in the eastern Kumtagh Desert (Dong et al., 2011).

3.3. Enrichment factors

Enrichment factors (EFs) were used to identify the elemental composition of surface material compared to crustal material. Al was used as the reference element in this paper. An EF value close to 1 was taken as an indication of crustal origin, whereas an EF value > 10 was considered to be an indication of anthropogenic sources (Zarasvandi et al., 2011; Jaafar et al., 2014). For the transported dust material (1.5-m height), the EF values of Co, As, and Ce were larger than 1 and smaller than 10 at all sites, indicating that these elements originated from both crustal and anthropogenic sources (Fig. 5). This finding is similar to the results obtained for normalized enrichment (Section 3.2), which indicated that Co, Nd, and As were enriched compared to the UCC, primarily because of anthropogenic sources. Most trace elements, such as P, Ti, V, Ni, Rb, Sr, Y, Ba, and La had EF values smaller than 1 at all sites, indicating that these elements originated from crustal sources. Anthropogenic activity can greatly affect the composition of Cl, Cr, Cu, and Zn. At Site 5, for example, which was downwind from a factory, the EF values for Cl, Cr, Cu, and Zn at the surface were primarily smaller than 1. However, these values were larger than 1 at a height of 1.5 m, particularly for Cl, which had a value larger than 10 (Fig. 5).

Table 3
Correlation matrix of 28 geochemical elements at six sites.

	Site 1	Site 2	Site 3	Site 4	Site 5	Site 6
Site 1	1					
Site 2	0.996	1				
Site 3	0.995	0.992	1			
Site 4	0.982	0.966	0.968	1		
Site 5	0.476	0.412	0.424	0.628	1	
Site 6	0.792	0.744	0.755	0.889	0.914	1

For the major oxides, all EF values were smaller than 10, indicating that these elements originated from both crustal and anthropogenic sources (Fig. 6). The EF values of Al_2O_3, Fe_2O_3, and K_2O were smaller than 1 at all sites, indicating that these elements came from crustal sources. SiO_2 clearly originated from crustal sources, and the EF values of SiO_2 were influenced by surface sand availability. In agreement with a study by Dong et al. (2011) conducted in the Kumtagh Desert, the EF values for SiO_2 were larger than 1 in the sandy desert (Sites 1 and 2 in this paper) but were smaller than 1 in the gravel desert without rich sand (Sites 2, 3, 4 and 5 in this paper). The value for Na_2O was less than or equal to 1 except at Site 5 (1.14), indicating that Na_2O originated from crustal sources in most of the sandy and gravel deserts of China, where there was no anthropogenic activity. MgO arose from a crustal source at Sites 1 and 2 and from both crustal and anthropogenic sources at Sites 3, 4, 5, and 6.

4. Discussion

4.1. Geochemical composition of the transported dust and surface

A previous study has indicated that abrasion and sorting during transportation can affect the geochemical composition of siliciclastic deposits (Nesbitt and Young, 1996). Wind sorting is an important factor in the sand transport process, and smaller grain sizes have a weak effect on sorting (Zhang and Dong, 2014b). However, for dust emission, there have been almost no studies on differences between the surface geochemical composition and the geochemical composition of transported dust materials. Fig. 7 shows the ratio of dust material from a height of 1.5 m to the surface dust material < 0.063 mm in size. Dust transport processes affected the composition of Fe_2O_3, MgO, and CaO, and these elements were depleted at a height of 1.5 m compared to the surface. However, Na_2O was enriched at a height of 1.5 m compared to the

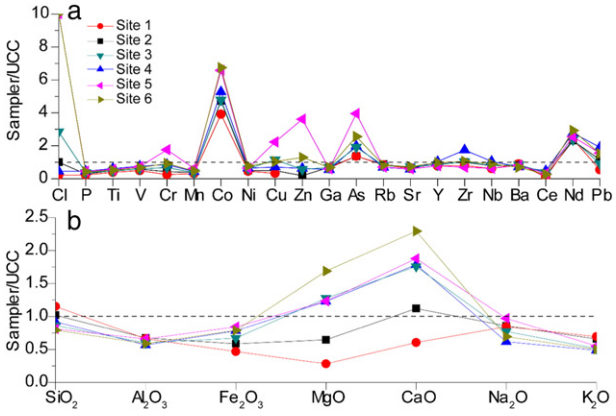

Fig. 4. Normalized major and trace elements at a height of 1.5 m at six sites.

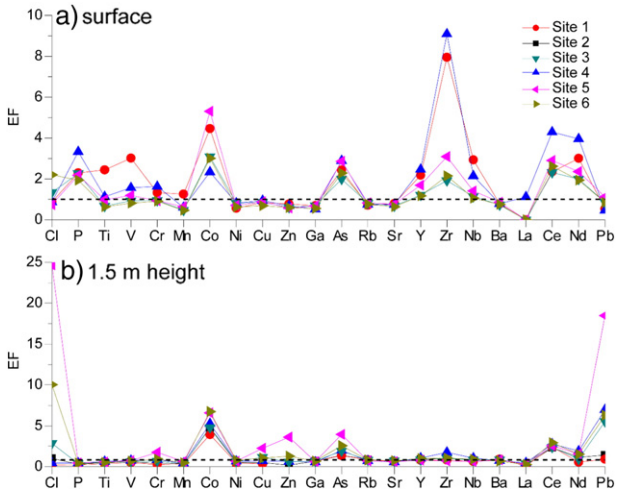

Fig. 5. EF values of trace elements at the surface (a) and at a height of 1.5 m (b).

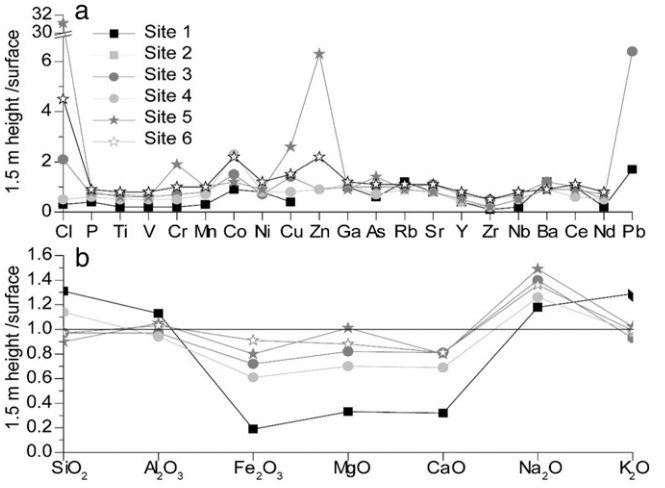

Fig. 7. Ratio of elemental composition between the surface and a height of 1.5 m for trace elements (a) and major elements (b).

surface (Fig. 7). SiO_2 was enriched for the gravel surface with sand and depleted for the gravel surface without crust, whereas Al_2O_3 and K_2O were enriched for the gravel with sand and the gravel without crust (Fig. 6a).

The trace element contents (P, Ti, V, Mn, Y, Zr, Nb, and Nd), which include the four main transported elements (P, Ti, Mn, and Zr), were depleted at a height of 1.5 m compared to the surface at all observation sites. Cr, Cu, Zn, and As were obviously enriched at Site 6 compared to the other sites, indicating that anthropogenic activity affected these elements.

At present, most studies have used EF values to identify dust sources (Jaafar et al., 2014; Li et al., 2014; Zhang and Dong, 2014b). However, from our geochemical analysis (Figs. 6, 7), we found that the EF values were different for land surfaces and transported materials (at 1.5 m in height), which is similar to the results of Cesari et al. (2012). At all sites, although the EF values of the trace elements (P, Co, As, Y, Zr, Nb, Ce, Nd, and CaO) were larger than 1 at the surface, only the EF values of Co, As, and Ce were larger than 1 at a height of 1.5 m. For the major oxides, all EF values were smaller than 10. Almost all of the trace elements had EF values of <10 except for Co; the EF values of Co were larger than 10 for the sub-regions b and c and ranged from 1 to 10 for the sub-regions a, d and e. At the land surface, the EF values of P, Co, As, Y, Zr, Nb, Ce, Nd, and CaO were larger than 1 at all sites. However, at a height of 1.5 m, the EF values for As and Ce, like Co, were larger than 1 at all sites. The most prominent change in elemental composition was observed for Nd, which was affected by the dust emission process. The normalized enrichment showed that Nd was enriched (Fig. 4), and the EF values at the surface and at a height of 1.5 m showed that this element originated from both crustal and anthropogenic sources (Fig. 5). However, the ratio of the EF values at a height of 1.5 m and at the surface showed that this element was depleted (Fig. 7b).

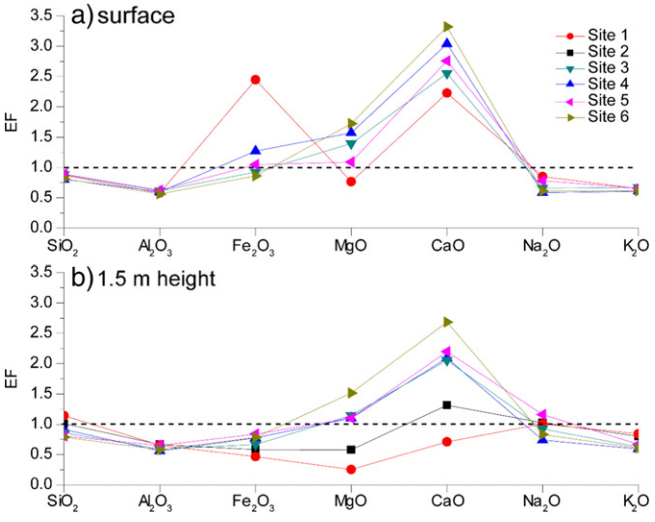

Fig. 6. EF values of major elements at the surface (a) and at a height of 1.5 m (b).

A previous study has used the Ca content as a tracer to identify dust sources. In a study by Li et al. (2014), the CaO content in Xi'an city (located in Loss) has been compared to that in Yulin city (also in Loss), and the authors have found that the Ca can be used as a tracer index to identify dust sources. From our geochemical analysis, we found that the content of CaO was greater than that of the UCC for almost all sites (except Site 1, Fig. 4). However, we must note that dust emission and transport processes resulted in depletion of the CaO content (Figs. 6, 7), which indicates that the higher Ca content occurring downwind of dust sources must have mixed with anthropogenic sources during transportation. Therefore, based on this result, the surface sediment composition must be considered in identifying dust sources.

4.2. Identification of dust sources by elemental tracers

Most aeolian and atmospheric research suggests that the northwestern Chinese deserts and the Gobi Desert are dust sources (Zhang et al., 1996; Zhang and Gong, 2005). However, there is no definitive answer regarding which land surfaces are the primary dust sources. We must note that in atmospheric research, there is no standard method for identifying dust sources. Previous studies have used different geochemical methods to identify dust sources. In Zhang et al. (1996) and Zarasvandi et al. (2011), four elements (Al, Fe, Mg and Sc) and the ratios of Fe/Al, Mg/Al, and Ca/Al were used to identify dust sources. In regard to the Ca/Al ratio, Wang et al. (2011) have found ratios of over 1.50 and 1.76 in the Taklimakan and 0.5 in the Gobi Desert (located in Mongolia and Inner Mongolia); Zhang et al. (2003b) have found a ratio of 0.94 in Dunhuang; Wang et al. (2011) have found a ratio of 1.26 in Loss; and Li (2009) have found a ratio of 0.68 in Beijing. Therefore, we propose that the sand and gravel desert in northwest China is the dust source. In this paper, we reproduced a previous study of Ca/Al in dust sources and deposition areas and demonstrated their population distributions (Fig. 8). In the source regions, such as the Kumtagh Desert and the adjacent gravel desert, the Hexi Corridor sandy desert, the Hexi Corridor gravel desert, the Badain Jaran Desert, and the Tengger Desert, the values of the Ca/Al ratio ranged from 0.1 to 1.0. However, the values of the Ca/Al ratio were larger than 1 at the Tarim Basin, which is similar to the results of previous studies by Zhang et al.

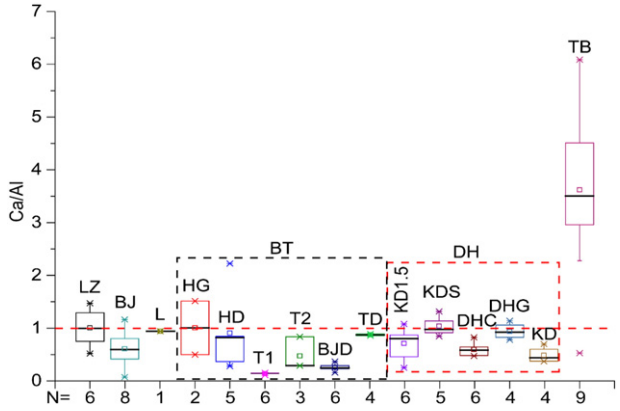

Fig. 8. Boxplots of Ca/Al in dust sources (Badain Jaran Desert, Tengger Desert, Hexi Corridor sandy and gravel desert, Kumtagh Desert and adjacent gravel desert, and Tarim Basin) and deposition regions (Lanzhou city, Loss, and Beijing). Lanzhou (LZ, Liu, 2012; Shi et al., 1995; Liu et al., 2004), Dunhuang (DHC, Zhang et al., 1997; Liu et al., 2004; Ta et al., 2003), Hexi Corridor Desert (HD, Zhang et al., 1997; Ta et al., 2003), Hexi Corridor Desert (HG, Ta et al., 2003), Tengger Desert (T1, Li, 2011), Tengger Desert (T2, Zhang et al., 1997; Liu et al., 2002), Tengger Desert deposition (TD, Zhang and Dong, 2014a), Loss (L, Zhang et al., 1997; Zhang et al., 2003b), Badain Jaran Desert (BJD, Li, 2011), Dunhuang gravel desert (DHG, Luo et al., 2014), Kumtagh sand desert (KD, Dong et al., 2011), Tarim Basin (TB, Honda et al., 2004), Beijing (BJ, Li, 2009), and the surface (KDS) and transported dust (KD1.5) evaluated in this study at the sandy desert adjacent to Dunhuang and the Gobi Desert regions. BT indicates the Badain Jaran Desert and the Tengger Desert; DH indicates Dunhuang and the adjacent sandy and gravel desert.

(1997) and Sun et al. (2005). Our results indicated similar spatial distributions of the Ca/Al ratio for the deposition region (Lanzhou, Beijing, Loss, and Tengger Desert), BT region (Badain Jaran Desert, Tengger Desert, Hexi Corridor Desert), and DH region (Dunhuang sandy and gravel desert). Therefore, it was difficult to identify the actual dust sources.

Therefore, we summarized the indices that are most frequently used (Rb/Sr and Ba/Sr) in research on dust sources (Fig. 9). We also used the ternary relationship between Fe/Al, Mg/Al, and Ca/Al (Fig. 10) to identify dust sources, which has been used to identify dust sources in the Mojave Desert in the southwestern USA (Sweeney et al., 2013). Based on our analysis of the data and published papers, we found that the relationship between Rb/Sr and Ba/Sr and the relationship between Fe/Al,

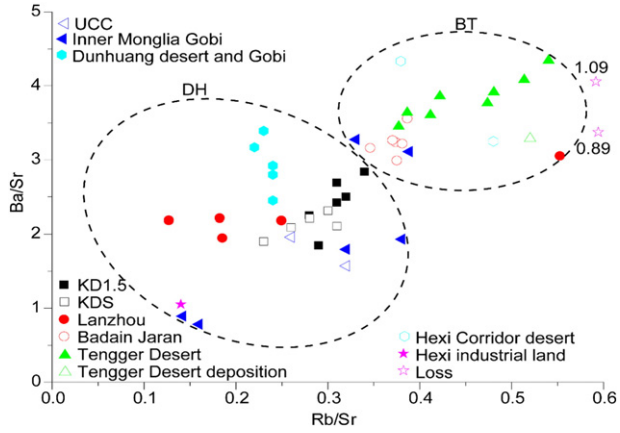

Fig. 9. Relationship between Rb/Sr and Ba/Sr. Lanzhou (Liu, 2012; Shi et al., 1995; Liu et al., 2004), Dunhuang (Zhang et al., 1997; Liu et al., 2004; Ta et al., 2003), Hexi Corridor Desert (Zhang et al., 1997; Ta et al., 2003), Hexi Corridor Desert (Ta et al., 2003), Hexi industrial land (Ta et al., 2003), Tengger Desert (Zhang et al., 1997; Liu et al., 2002; Li, 2011), Tengger Desert deposition (Zhang and Dong, 2014a), Loss (Zhang et al., 1997; Zhang et al., 2003a, 2003b), Badain Jaran (Zhang et al., 1997; Li, 2011; Luo et al., 2014), Inner Mongolian Gobi (Luo et al., 2014), UCC (Taylor and McLennan, 1995), and the surface (KDS) and transported dust (KD1.5) evaluated in this study at the sandy desert adjacent to the Dunhuang adjacent sandy and Gobi Desert regions. BT indicates the Badain Jaran Desert and the Tengger Desert; DH indicates Dunhuang and the adjacent sandy and gravel desert. The data shown by empty stars indicate the Rb/Sr values.

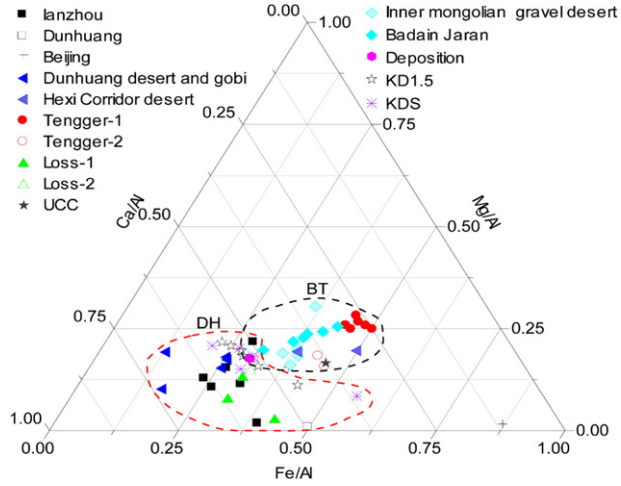

Fig. 10. Ternary relationships between Fe/Al, Mg/Al, and Ca/Al. UCC (Taylor and McLennan, 1995), deposition (Zhang and Dong, 2014a), Loss-2 (Liu et al., 2002), Tengger-2 (Ta et al., 2003; Zhang et al., 1997; Liu et al., 2002), Hexi Corridor Desert (Ta et al., 2003; Zhang et al., 1997), Inner Mongolian gravel desert (Luo et al., 2014), Badain Jaran (Li, 2011), Beijing (Liu et al., 2004; Li, 2009), Loss-1 (Zhang et al., 1997, 2003b; Liu et al., 2004), Tengger-1 (Li, 2011), Hexi gravel desert (Ta et al., 2003), Dunhuang (Zhang et al., 1997; Liu et al., 2004), Lanzhou (Liu et al., 2004), and KD1.5 (transported dust at a height of 1.5 m) and KDS (surface) in the present study.

Mg/Al, and Ca/Al can be used to identify dust sources (Figs. 9, 10). Dust sources in northwestern China can be divided into two regions: the first region is the Badain Jaran Desert, Tengger Desert, Hexi Corridor Desert, and part of the Inner Mongolian Gobi Desert (denoted as BT, Badain Jaran Desert and Tengger Desert); and the second region is the desert adjacent to Dunhuang, Gobi Desert, and part of the Inner Mongolian Gobi Desert (denoted as DH, Dunhuang sandy and gravel desert).

4.3. Identification of dust sources by transported materials

The sandy and gravel desert in northwestern China is a major dust source. However, detailed information on the quantity of dust emission from the sandy and gravel desert has been lacking until now. Based on our field observations, we found that the quantity of dust emission (defined as $Q_{<63} = Q \times$ ratio of <63 μm sediment at a height of 1.5 m) over gravel with sand was the highest (mean = 253.01 g m^{-1} d^{-1}), followed by gravel without crust (mean = 109.16 g m^{-1} d^{-1}), and gravel with crust (mean = 61.977 g m^{-1} d^{-1}), while the lowest value was observed for sandy desert (mean = 2.07 g m^{-1} d^{-1}).

PCA can be used to extract factors after an analysis of ambient data that are associated with different source categories. Table 4 shows the

Table 4
Principal component analysis for the 22 trace and 7 major elements in transported sediments at a height of 1.5 m (n = 6). The table shows the principal components (PCs) with eigenvalues > 1. High positive values (>0.6) are shown in bold.

	PC1	PC2		PC1	PC2
Cl	**3.059**	**4.785**	Zr	−0.126	−0.269
P	**0.643**	−0.171	Nb	−0.842	−0.105
Ti	**10.568**	−1.474	Ba	**1.011**	−0.462
V	−0.661	−0.121	La	−0.814	−0.104
Cr	−0.659	−0.044	Ce	−0.628	−0.131
Mn	**1.013**	−0.133	Nd	−0.806	−0.102
Co	−0.561	−0.107	Pb	−0.588	0.036
Ni	−0.778	−0.105	SiO_2	−0.645	−0.155
Cu	−0.795	−0.076	Al_2O_3	−0.842	−0.105
Ga	−0.835	−0.106	Fe_2O_3	−0.865	−0.100
As	−0.844	−0.096	MgO	−0.869	−0.099
Rb	−0.636	−0.140	CaO	−0.855	−0.098
Sr	−0.097	−0.208	Na_2O	−0.866	−0.101
Y	−0.809	−0.110	K_2O	−0.870	−0.101

results of PCA for the transported dust material at a height of 1.5 m. Our PCA results indicated that two principal components (PCs) with eigenvalues >1 could be extracted from the data; these PCs explained 84.0% of the total variance. PC1 included Cl, P, Ti, Mn, and Ba (based on a high loading of 0.6, as described by Wang et al., 2012). Ti, Mn, P, and Ba came from crustal sources, whereas Cl was probably related to both crustal and anthropogenic sources. For PC2 (which explains 15.9% of the variance), there were no elements with loadings > 0.60, indicating that the sources of those elements were complex.

The spatial distribution of geochemical composition led to differences in the dust material elements. For example, Zhang et al. (2003a) have found that the main dust elements in the northern China desert included Al, Ca, Fe, K, Mn, Si and Ti. However, in this study, we found that the transported material primarily consisted of Ti, Cl, Mn, Ba, P, Sr, and Zr for the trace elements (the average contents were 46.1, 17.6, 7.7, 7.6, 6.1, 3.1, and 3.0%, respectively) and SiO_2, Al_2O_3, and CaO for the major elements (the average contents were 69.1, 10.8, and 7.7%, respectively). Although the contents of Al, Ca, Fe, Mn, Si and Ti were similar in northern and northwestern China, the contents of Ba, P, Cl, Sr, and Zr were higher in northwestern China.

4.4. Identification of dust sources by transport winds

The sand transport direction also influenced the dust transport direction. A previous study has indicated that the Hexi Corridor Desert is affected by the Mongolia–Siberia high-pressure system that occurs in late spring and early summer (Wang et al., 2005). Because of the obstruction of the western Qilian Mountains, the wind is divided into two branches: one crosses through the middle and southeastern area of the Hexi Corridor Desert and even reaches the Loss and Southeast China; the other crosses through the entire area of the northwestern Hexi Corridor Desert (mainly Dunhuang and the adjacent regions, Wang et al., 2005; Dong et al., 2011; Zhang et al., 2015). Fig. 10 shows that the Rb/Sr and Ba/Sr values at the Loss are similar to those of the BT region but different from those at the DH region, indicating that the BT region provided dust material for the Loss formation as well as modern dust material.

5. Conclusion

Dust geochemical compositions and the relationship between Rb/Sr and Ba/Sr, and between Fe/Al, Mg/Al, and Ca/Al can be used to identify dust sources. Based on our field observations and geochemical analysis, we found that the dust sources in northwestern China include two regions: one region is the Badain Jaran Desert, Tengger Desert, Hexi Corridor Desert, and part of the Inner Mongolian Gobi Desert; the other region is the desert adjacent to Dunhuang, Gobi Desert, and part of Inner Mongolian Gobi Desert (denoted as DH, Dunhuang sandy and gravel desert).

Ti, Mn, Ba, P, Cl, Sr, and Zr were the primary trace elements that were transported and accounted for >90% of the total trace elements. Ti, Mn, Ba, and Sr were depleted compared to the UCC. Based on the EF values and the PCA method, Ti, P, Ba, and Sr originated from crustal sources and Cl originated from both crustal and anthropogenic sources.

Dust transport processes affect the geochemical properties of dust. Only 3 of the EF values (Co, As, and Ce) for the transported dust material were larger than 1 at all sites, whereas 9 elements (P, Co, As, Y, Zr, Nb, Ce, Nd, and CaO) had EF values larger than 1 for all site surfaces.

Acknowledgments

We gratefully acknowledge funding from the Youth Innovation Promotion Association of the Chinese Academy of Sciences (CAS), Technology of the People's Republic of China (2013CB956000) and the West Light Foundation of the Chinese Academy of Sciences (CAS). We also express appreciation to the journal's reviewers for their invaluable comments on improving the manuscript.

Appendix A. Supplementary data

Supplementary data to this article can be found online at http://dx.doi.org/10.1016/j.gexplo.2016.11.006.

References

Abouchami, W., Näthe, K., Kumar, A., Galer, S.J.G., Jochum, K.P., Williams, E., Horbe, A.M.C., Rosa, J.W.C., Balsam, W., Adams, D., Mezger, K., Andreae, M.O., 2013. Geochemical and isotopic characterization of the Bodélé Depression dust source and implications for transatlantic dust transport to the Amazon Basin. Earth Planet. Sci. Lett. 380, 112–123.
Arimoto, R., 2001. Eolian dust and climate: relationships to sources, tropospheric chemistry, transport and deposition. Earth-Sci. Rev. 54, 29–42.
Cesari, D., Contini, D., Genga, A., Siciliano, M., Elefante, C., Baglivi, F., Daniele, L., 2012. Analysis of raw soils and their re-suspended PM10 fractions: characterisation of source profiles and enrichment factors. Appl. Geochem. 27, 1238–1246.
Dong, Z.B., Su, Z.Z., Qian, G.Q., Luo, W.Y., Zhang, Z.C., Wu, J.F., 2011. Aeolian Geomorphology of the Kumtagh Desert. Science Press, Beijing.
Du, R.H., 1962. The characteristics of the Hexi Corridor northwest gravel desert. The Sinica of the 1960' National Conference on the Geography, pp. 256–266 (in Chinese).
Honda, M., Yabuki, S., Shimizu, H., 2004. Geochemical and isotopic studies of aeolian sediments in China. Sedimentology 51, 211–230.
Jaafar, M., Baalbaki, R., Mrad, R., Daher, N., Shihadeh, A., Sioutas, C., Saliba, N.A., 2014. Dust episodes in Beirut and their effect on the chemical composition of coarse and fine particulate matter. Sci. Total Environ. 496, 75–83.
Kok, J.F., Parteli, E.J.R., Michaels, T.I., Bou, K.D., 2012. The physics of wind-blown sand and dust. Report Prog. Physics. 75, p. 106901.
Li, J., 2009. Characteristics, Source, Long-range Transport of Dust Aerosol over the Central Asia and its Potential Effect on Global Change. Fudan University (in Chinese).
Li, E.J., 2011. Comparison Research on the Badain Jaran Desert and Tengger Desert Sediment Characteristics. Shanxi Normal University (in Chinese).
Li, X.P., Feng, L.N., Huang, C.C., Yan, X.Y., Zhang, X., 2014. Chemical characteristics of atmospheric fallout in the south of Xi'an during the dust episodes of 2001–2012 (NW China). Atmos. Environ. 83, 109–118.
Liu, J., 2012. Study on the Source and Characteristics of Grain Size Distribution of Atmospheric Dust Fall in Lanzhou. Lanzhou University (in Chinese).
Liu, C.L., Zhang, J., Liu, S.M., 2002. Physical and chemical characters of materials from several mineral aerosol sources in China. Environ. Sci. 23 (4), 28–32.
Liu, W., Feng, Q., Wang, T., Zhang, Y.W., Shi, J.H., 2004. Physicochemistry and mineralogy of storm dust and dust sediment in northern China. Adv. Atmos. Sci. 21, 775–783.
Nesbitt, H., Young, G., 1996. Petrogenesis of sediments in the absence of chemical weathering: effects of abrasion and sorting on bulk composition and mineralogy. Sedimentology 43, 341–358.
Pye, K., 1987. Aeolian Dust and Dust Storms. Academic Press, Gainesville.
Reheis, M.C., Budahn, J.R., Lamothe, P.J., 2002. Geochemical evidence for diversity of dust sources in the southwestern United States. Geochim. Cosmochim. Acta 66, 1569–1587.
Shi, Y.X., Dai, X.R., Li, J.T., Xue, B., 1995. On the wind-blown deposits from a heavy dustfall numbered "930505" in Lanzhou, North-central China. Ac. Sedimentol. Sinica 13, 76–82 (In Chinese).
Sun, Y., Zhuang, G., Wang, Y., Zhao, X., Li, J., Wang, Z., An, Z., 2005. Chemical composition of dust storms in Beijing and implications for the mixing of mineral aerosol with pollution aerosol on the pathway. J. Geophys. Res. 110, D24209.
Sweeney, M.R., McDonald, E.V., Markley, C.E., 2013. Alluvial sediment or playas: what is the dominant source of sand and silt in desert soil vesicular A horizons, southwest USA. J. Geophys. Res. Earth Surf. 118, 257–275.
Ta, W.Q., Xiao, Z., Qu, J.J., Yang, G.S., Wang, T., 2003. Characteristics of dust particles from the desert/Gobi area of northwestern China during dust-storm periods. Environ. Geol. 43, 667–679.
Taylor, S.R., McLennan, S.M., 1995. The geochemical evolution of the continental crust. Rev. Geophys. 33, 241–265.
Wang, X.M., Dong, Z.B., Yan, P., Yang, Z., Hu, Z.X., 2005. Surface sample collection and dust source analysis in northwestern China. Catena 59, 35–53.
Wang, Q.Z., Zhuang, G.S., Li, J., Huang, K., Zhang, R., Jiang, Y.L., 2011. Mixing of dust with pollution on the transport path of Asian dust — revealed from the aerosol over Yulin, the north edge of Loess Plateau. Sci. Total Environ. 409, 573–581.
Wang, X.M., Xia, D.S., Zhang, C.X., Lang, L.L., Hua, T., Zhao, S., 2012. Geochemical and magnetic characteristics of fine-grained surface sediments in potential dust source areas: implications for tracing the provenance of aeolian deposits and associated palaeoclimatic change in East Asia. Palaeogeogr. Palaeoclimatol. Palaeoecol. 323-325, 123–132.
Zarasvandi, A., Carranza, E.J.M., Moore, F., Rastmanesh, F., 2011. Spatio-temporal occurrences and mineralogical–geochemical characteristics of airborne dusts in Khuzestan Province (southwestern Iran). J. Geochem. Explor. 111, 138–151.
Zhang, Z.C., Dong, Z.B., 2014a. Effect of dust deposition collection method on dust physicochemical properties and its environmental significance. China Environ. Sci. 34, 3034–3040 (In Chinese).
Zhang, Z.C., Dong, Z.B., 2014b. The characteristics of aeolian transport particle size distribution over the artificial pebble surfaces. J. Desert Res. 34, 639–644 (in Chinese).

Zhang, X.Y., Gong, S.L., 2005. Contribution of the anthropogenic desertification in China to Asian dust storm. Adv. Clim. Chang. Res. 1 (4), 147–150 (in Chinese).
Zhang, X.Y., Zhang, G.Y., Zhu, G.H., Zhang, D.E., An, Z.S., Chen, T., Huang, X.P., 1996. Elemental tracers for Chinese source dust. Sci. China Ser. D 39, 512–521.
Zhang, X.Y., Arimoto, R., An, Z.S., 1997. Dust emission from Chinese desert sources linked to variations in atmospheric circulation. J. Geophys. Res. 102, 28041–28047.
Zhang, X.Y., Gong, S.L., Arimoto, R., Shen, Z.X., Mei, F.M., Wang, D., Cheng, Y., 2003a. Characterization and temporal variation of Asian dust aerosol from a site in the northern Chinese deserts. J. Atmos. Chem. 44, 241–257.
Zhang, X. Y., Gong, S. L., Shen, Z. X., Mei, F. M., Xi, X. X., Liu, L.C., Zhou, Z. J., Wang, D., Wang, Y. Q., Cheng, Y., 2003b. Characterization of soil dust aerosol in China and its transport and distribution during 2001 ACE-Asia: 1. Network observations. J. Geophys. Res. 108, NO. D9, 4261.
Zhang, Z.C., Dong, Z.B., Zhao, A.G., 2011. The characteristics of aeolian sediment flux profiles in the southeastern Tengger Desert. Sedimentology 58, 1884–1894.
Zhang, Z.C., Dong, Z.B., Li, C.X., 2015. Wind regime and sand transport in China's Badain Jaran Desert. Aeolian Res. 17, 1–13.
Zhang, Z.C., Dong, Z.B., Qian, G.Q., Li, J.Y., Jiang, C.W., 2016. Implications of surface properties for dust emission from gravel deserts (gobis) in the Hexi corridor. Geoderma 268, 69–77.